in Fig. 5, b and c, the areas of highest variability on the Wu-Kabat analysis correspond, in general, with hydrophilic regions of the molecule, consistent with these regions being available to interact with ligand. In addition, the hydrophilicity plot shows conservation of several hydrophobic regions, which are thought to be involved in the formation of a common tertiary structure shared among all TCR chains as well as members of the immunoglobulin supergene family (*4, 30*).

Pairwise comparison of the 15 human V_β genes in Figs. 1 and 4 with known murine V_β sequences does not present any clear picture of allelic evolutionary relationships. For example, human V_β genes ATL 12-2, ph 22, ph 16, HPB-MLT, ph 8, YT35, and ph 29 are all more homologous to the murine V_β11 gene than any other known murine V_β gene (54 to 68% at the amino acid level, 64 to 78% at the nucleotide level). Some of these genes are actually more homologous to the murine gene than they are to each other. Thus seven different human V_β genes representing three different subfamilies all show significant homology to the same murine V_β gene. In other cases, significant homology is found in only a single murine-human pairwise combination. ATL 12-1 is most homologous to the murine V_β3 gene (54% amino acid, 66% nucleotide), ph 24 is most homologous to the murine V_β5.2 gene (55% amino acid, 65% nucleotide), and ph 34 and Molt 4 are most homologous to the murine V_β15 gene (47% amino acid, 64% nucleotide). When pairwise comparisons between the most homologous murine and human V_β genes are aligned together, amino acid substitutions are seen to occur more often in hydrophilic regions of the molecule, and the frequency of these substitutions roughly parallels the plot of V_β variability in general. In these cases, therefore, evolution of V_β alleles between species is similar to the evolution of nonallelic V_β genes within a species, with changes being concentrated in the hydrophilic regions of the molecule.

Note added in proof: Similar results have been obtained by Kimura *et al.* (*31*).

REFERENCES AND NOTES

1. O. Acuto *et al.*, *Cell* **34**, 717 (1983).
2. J. Kappler, R. Kubo, K. Haskins, J. White, P. Marrack, *ibid.*, p. 727.
3. B. W. McIntyre and J. P. Allison, *ibid.*, p. 739.
4. J. Novotny, S. Tonegawa, H. Saito, D. Kranz, H. Eisen, *Proc. Natl. Acad. Sci. U.S.A.* **83**, 742 (1986).
5. R. M. Zinkernagel and P. C. Doherty, *Nature (London)* **248**, 701 (1974).
6. G. M. Shearer, *Eur. J. Immunol.* **4**, 527 (1974).
7. P. Patten *et al.*, *Nature (London)* **312**, 40 (1984).
8. R. Barth *et al.*, *ibid.* **316**, 517 (1985).
9. M. Behlke *et al.*, *Science* **229**, 566 (1985).
10. M. Behlke, H. S. Chou, K. Huppi, D. Y. Loh, *Proc. Natl. Acad. Sci. U.S.A.* **83**, 767 (1986).
11. K. Ikuta, T. Ogura, A. Shimizu, T. Honjo, *ibid.* **82**, 7701 (1985).
12. N. Jones *et al.*, *Science* **227**, 311 (1985).
13. A. Tunnacliffe, R. Kefford, C. Milstein, A. Forster, T. H. Rabbitts, *Proc. Natl. Acad. Sci. U.S.A.* **82**, 5068 (1985).
14. G. Siu *et al.*, *Cell* **37**, 395 (1984).
15. Y. Yanagi *et al.*, *Nature (London)* **308**, 145 (1984).
16. M. Weigert, R. Riblet, *Cold Spring Harbor Symp. Quant. Biol.* **41**, 839 (1977).
17. M. Abramowitz and I. A. Stegun, *Handbook of Mathematical Functions* (National Bureau of Standards Applied Mathematics Series No. 55, Government Printing Office, Washington, DC, 1970).
18. A maximum likelihood estimate of $n = 21$ was obtained by determining the value of n that maximized $P(d)$ for d and r fixed at $d = 14$ and $r = 22$. A 95% one-sided confidence bound of $n = 40$ was obtained by determining the smallest value of n for which the probability of observing at most 14 different segments among 22 segments examined was less than 0.05.
19. S. Tonegawa, *Nature (London)* **302**, 575 (1983).
20. B. Toyonaga, Y. Yoshikai, V. Vadasz, B. Chin, T. W. Mak, *Proc. Natl. Acad. Sci. U.S.A.* **82**, 8624 (1985).
21. L. Hood, J. H. Campbell, S. C. R. Elgin, *Annu. Rev. Genet.* **9**, 305 (1975).
22. D. Becker *et al.*, *Nature (London)* **317**, 430 (1985).
23. Y. Chien *et al.*, *ibid.* **312**, 31 (1984).
24. H. Saito *et al.*, *ibid.*, p. 36.
25. E. A. Kabat, T. T. Wu, H. Bilofsky, M. Reid-Miller, H. Perry, *Sequences of Proteins of Immunological Interest* (National Institutes of Health, Bethesda, MD, 1983).
26. L. M. Amzel and R. J. Poljak, *Annu. Rev. Biochem.* **48**, 961 (1979).
27. D. R. Davies and H. Metzger, *Annu. Rev. Immunol.* **1**, 87 (1983).
28. T. Wu and E. Kabat, *J. Exp. Med.* **132**, 211 (1970).
29. T. P. Hopp and K. R. Woods, *Proc. Natl. Acad. Sci. U.S.A.* **78**, 3824 (1981).
30. J. Novotny and E. Haber, *ibid.* **82**, 4592 (1985).
31. N. Kimura, B. Toyonaga, Y. Yoshikai, T. Mak, *J. Exp. Med.*, in press.
32. T. V. Huynh, R. A. Young, R. N. Davis, in *DNA Cloning: A Practical Approach*, D. Glover, Ed. (IRL Press, Oxford, 1984), pp. 49–78.
33. R. Epstein *et al.*, *J. Exp. Med.* **161**, 1219 (1985).
34. A. Maxam and W. Gilbert, *Proc. Natl. Acad. Sci. U.S.A.* **74**, 560 (1977).
35. F. Sanger, S. Nicklen, A. Coulsen, *ibid.*, p. 5463.
36. M. D. Biggin, T. J. Gibson, G. F. Hong, *ibid.* **80**, 3963 (1983).
37. G. I. Bell *et al.*, *ibid.* **78**, 5759 (1981).
38. E. M. Southern, *J. Mol. Biol.* **98**, 503 (1975).
39. T. Maniatis, E. Fritsch, J. Sambrook, *Molecular Cloning: A Laboratory Manual* (Cold Spring Harbor Laboratory, Cold Spring Harbor, NY, 1982).

40. We thank Dr. Daniel Hartl for assistance with the statistical analysis and Madline Pearlman for manuscript preparation. Supported by funds from the Howard Hughes Medical Institute (D.Y.L.), NIH training grant 2-T32-AI00112 (J.P.T.), and National Institute of Health Research Service Award, GM 07200, Medical Scientist Training Program, from the National Institute of General Medical Sciences (M.A.B.).

3 March 1986; accepted 6 June 1986

Replication of the B19 Parvovirus in Human Bone Marrow Cell Cultures

KEIYA OZAWA,* GARY KURTZMAN, NEAL YOUNG

The B19 parvovirus is responsible for at least three human diseases. The virus was successfully propagated in suspension cultures of human erythroid bone marrow from patients with hemolytic anemias; release of newly synthesized virus into the supernatants of infected cultures was observed. This culture system allowed study at a molecular level of events associated with the B19 life cycle. The B19 parvovirus replicated through high molecular weight intermediate forms, linked through a terminal hairpin structure. B19 replication in vitro was highly dependent on the erythropoietic content of cultures and on addition of the hormone erythropoietin.

THE B19 PARVOVIRUS WAS DISCOVERED in the sera of normal blood donors in 1975 (*1*) and subsequently was identified as the causative agent of (i) transient aplastic crisis of hemolytic disease (*2*), (ii) the common childhood exanthem called fifth disease (*3*), and (iii) a polyarthralgia syndrome in normal adults (*4*). In addition, B19 parvovirus may be responsible for some cases of hydrops fetalis (*5*). The genome of the B19 virus consists of about 5.4 kb of single-stranded DNA (*6–8*), which encodes at least two capsid proteins of about 84 and 58 kD (*9, 10*). Genetic studies have been hampered by the inability to propagate the B19 parvovirus in vitro. Even though B19-containing sera are potent inhibitors of colony formation by bone marrow erythroid progenitor cells (*11*), clonogenic assays are inadequate for either maintenance or molecular study of the B19 virus. We report here successful propagation of B19 parvovirus in a tissue culture system by means of fresh human bone marrow cells.

Serum containing B19 parvovirus (Minor II, 60 μg of B19 DNA per milliliter) was obtained from a patient with sickle cell disease and transient aplastic crisis during a recent B19 epidemic (*12*). It was adsorbed to erythroid bone marrow mononuclear cells that had been obtained with informed consent from patients with hemolytic anemias; the infected cells were then grown in standard growth medium in the presence of the erythroid cell–specific hormone erythropoietin. Virus addition only slightly de-

Cell Biology Section, Clinical Hematology Branch, National Heart, Lung, and Blood Institute, Bethesda, MD 20892.

*To whom communications should be addressed at ACRF 7C108, National Institutes of Health, Bethesda, MD 20892.

creased the total cell number after 9 days of culture but markedly reduced the number of erythroid precursor cells (erythroblasts and normoblasts) from 70% at initiation of culture to less than 10% of total cells. In uninfected control cultures, the combination of an increase in total cell number and a slight decrease in erythroid cell number resulted in a decrease in the proportion of erythroid cells to about 50% after 1 week of incubation.

Table 1. Dependence of parvovirus replication on erythropoietic activity. Erythroid bone marrow was obtained from patients with sickle cell disease; myeloid bone marrow was from a patient with a myeloproliferative disorder with large numbers of granulocyte-macrophage progenitors (CFU-C) but no burst-forming units (BFU-E) or erythroid colony-forming units (CFU-E) in clonal assay. Abbreviations: *n*, number of samples examined; Epo, erythropoietin; HPCM, human placental–conditioned medium; PHA-LCM, phytohemagglutinin-stimulated leukocyte-conditioned medium.

Relation to erythroid content of bone marrow samples				Relation to added hematopoietic factors		
Target cells	*n*	Erythroblast %	B19 copies per cell	Culture supplement	B19 copies per cell* Exp. 1	B19 copies per cell* Exp. 2
Erythroid	5	44–72	3000–5000	None	200	300
Normal	5	17–35	1000–2000	Epo (U/ml)		
Myeloid	1	0	0	0.1		800
				0.3		1250
				1.0	2000	1250
				3.0	2000	1200
				HPCM (10%)	500	550
				PHA-LCM (10%)		300

*Normal bone marrow target cells.

To detect B19 propagation, we analyzed DNA from whole cells, nuclei, and cytosol, as well as from supernatants of infected and control cultures by DNA hybridization with a B19-specific probe (Fig. 1). At 48 hours of culture, there was 20 times more B19 DNA in nuclei than in the cytosol; there was 10 times as much B19 DNA in whole cells as in supernatant. The average number of virus gene copies in the total bone marrow was about 3000 to 5000 per cell, based on comparison with standard B19 DNA (however, if the virus infection was located only within erythroid cells, the number of copies was 5000 to 8000 per infected cell).

To demonstrate release of newly synthesized B19 parvovirus from infected cells, we added [^{3}H]thymidine to cultures 24 hours after inoculation. Supernatants were harvested 3 days later for analysis of incorpo-

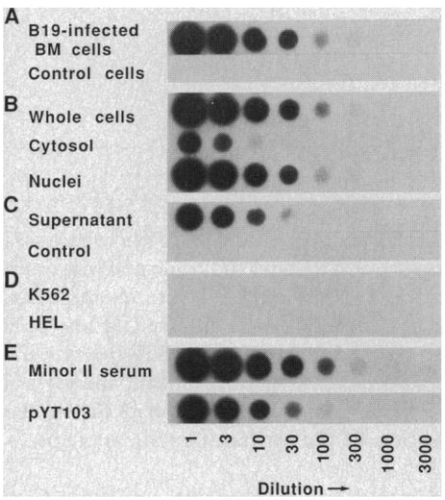

Fig. 1. Quantitation by dot blot analysis of B19 DNA. (A) Comparison of B19-infected and control uninfected erythroid bone marrow (BM) cultures. Ten microliters of serum containing B19 parvovirus was added to 5×10^7 mononuclear bone marrow cells in 1 ml of Iscove's modification of Dulbecco's medium (IMDM) (*16*). Cells and serum were incubated for 2 hours at 4°C, then diluted to 2×10^6 cells per milliliter in IMDM containing 20% fetal calf serum (FCS) and erythropoietin (1 U/ml; Connaught, step 3), and cultured at 37°C, 95% humidity, 5% CO_2. Control cultures lacked B19 serum. After 2 days of culture, DNA was extracted, and serial dilutions of 1 μg of alkaline-denatured DNA were applied to a minifold dot blot apparatus. Immobilized DNA on nitrocellulose filters was hybridized with nick-translated pYT103 (*17*) in 6× standard saline citrate (SSC), 0.5% SDS, 5× Denhardt's solution, denatured salmon sperm DNA (100 μg/ml). (B) B19 DNA in cytosol and nuclei. Nuclear and cytosol fractions were obtained by Dounce homogenization (*18*). Serial dilutions of DNA from 10^5 cells were applied to each lane. (C) B19 DNA in supernatants. Cells were washed to remove residual inoculum on day 1; after a further 3 days of culture, the quantity of B19 DNA extracted from 100 μl of supernatant was determined. The final wash medium was incubated to serve as a control. (D) B19 infection of erythroleukemia cell lines. K562 or HEL were infected as in (A); 10 μg of DNA and serial dilutions were applied to each lane. (E) Determination of input virus quantity. DNA from 0.1 μl of serum (Minor II) was applied in serial dilutions. Gene copy number was determined by comparison to 10^3 pg of pYT103 DNA.

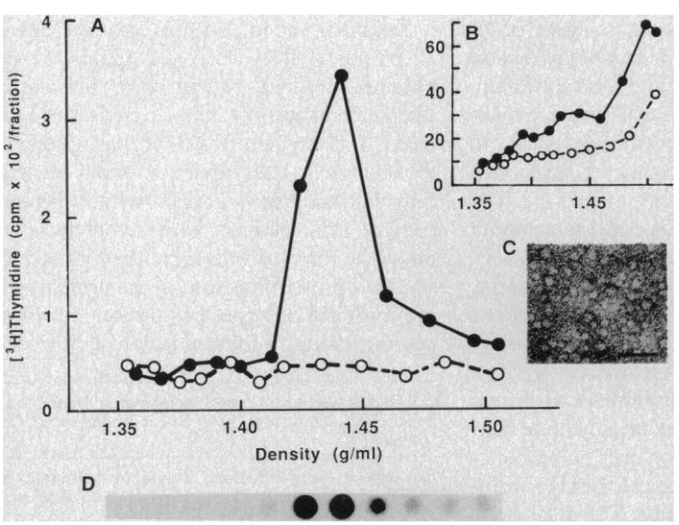

Fig. 2. Density gradient centrifugation of newly synthesized B19 parvovirus. Erythroid bone marrow cultures were exposed to serum containing B19 as described in the legend to Fig. 1. Twenty-four hours after inoculation, [^{3}H]thymidine (1 μCi/ml; specific activity, 6.7 Ci/mmol; New England Nuclear) was added to a total of 5×10^7 cells, and the cultures were incubated for an additional 72 hours before separation of supernatants from cells by centrifugation. Supernatants were concentrated by sedimentation through a cushion of 40% sucrose in phosphate-buffered saline (PBS) at 38,000 rev/min for 12 hours. After aspiration of liquid, the particulate fraction was suspended in PBS and digested with DNase I in the presence of Mg^{2+}. Volume was then adjusted to 5 ml with tris-EDTA buffer, and cesium chloride was added to a final concentration of 1.4 g/ml. A gradient was established by centrifugation at 35,000 rev/min for 26 hours in a Beckman SW 50.1 rotor. Sixteen fractions were removed from above and analyzed by scintillation counting for the presence of ^{3}H; the density of individual fractions was determined by refractometry (the four lightest fractions have been omitted for purposes of illustration). The pattern of radioactivity after immunoprecipitation of viral particles with human antiserum to B19 and protein A–Sepharose is shown in (A); total radioactivity is shown in the insert (B). An electron micrograph of the pooled peak fractions (1.42 to 1.46 g/ml) showed regular 24-nm particles characteristic of parvovirus (×95,000); scale bar, 100 nm (C). The B19 gene content of each fraction was determined by dot blot analysis with ^{32}P-labeled pYT103 (strip D).

ration of radioactive nucleotide into virion particles (Fig. 2). Radioactivity from infected culture supernatants sedimented in a broad band, with an apparent shoulder from 1.41 to 1.46 g/ml in cesium gradients (Fig. 2B), but immunoprecipitation of viral particles with antiserum to B19 showed a sharp peak at the expected density for parvoviruses, 1.42 to 1.45 g/ml (Fig. 2A) (*7*); B19 DNA, detected by dot blot analysis, was located in the same fractions (Fig. 2D). Electron microscopy showed characteristic parvovirus particles of 24-nm diameter in the pool of fractions from 1.42 to 1.46 g/ml from infected cultures (Fig. 2C) (*13*).

Replication forms of the B19 virus were detected in the nuclear DNA of infected bone marrow cells by three methods. First, DNA from infected cells, supernatants of infected cultures, or virions was rapidly extracted under low salt conditions to prevent annealing of the positive and negative strands, which are packaged separately in virions (*7*) (Fig. 3A). Under these conditions, all the B19 DNA present in virions migrated as single-stranded DNA. In contrast, some of the DNA extracted from the nuclei of infected cells migrated as larger size bands of 5.2 to 5.3 kb and 10.5 kb, corresponding to the monomeric and dimeric replication forms. Only single-stranded DNA was present in the cytosol and supernatants from infected cultures, consistent with the presence of the complete virions. These results indicated a nuclear replication site for B19 parvovirus.

Second, to discriminate replication forms from annealed duplexes, we extracted DNA, annealed positive and negative strands, and then subjected the DNA to restriction enzyme digestion and analysis by DNA hybridization (Fig. 3B). In undigested specimens, two differences were noted in the pattern of B19 parvovirus DNA from nuclei of infected cells compared to that from virions: the slightly lower molecular weight of the monomeric duplex (due to the presence of the hairpin form) and the presence of a 10.5-kb band (representing the dimer duplex). Digestion with Bam HI, which recognizes only a single site in B19 DNA, generated two fragments from annealed virion DNA of 3.9 and 1.5 kb. In contrast, Bam HI digestion of nuclear DNA resulted in doublets of 3.9 and 3.8 kb and of 1.5 and 1.4 kb, due to structural differences between hairpin and extended forms of the restriction fragments (Fig. 3B). The presence of equal quantities of DNA in each doublet indicated replication of B19 from both positive and negative strands. These data are consistent with the replication forms of B19 parvovirus generated by DNA polymerase in a cell-free system (*8*).

Third, the covalently linked hairpin structure of the replication forms was demonstrated by a "snap-back" procedure, in which DNA duplexes were sequentially subjected to heat, quick chilling, and treatment with mung bean nuclease (*8*) (Fig. 4). Heating of virion DNA denatures the annealed duplexes of positive and negative strands;

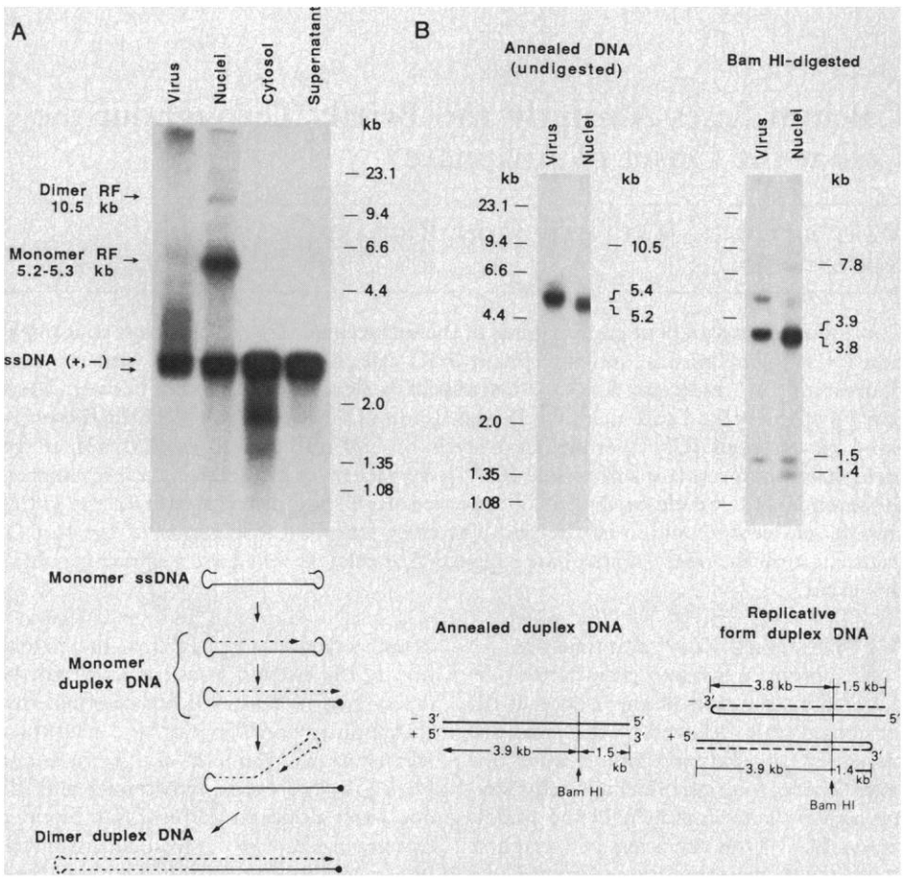

Fig. 3. Demonstration of B19 replicative forms in nuclei of infected bone marrow cells. (A) Agarose gel electrophoresis of B19 DNA from infected bone marrow cultures and virions (native forms). DNA was extracted under low salt conditions to prevent annealing of positive and negative strands in vitro (*8*). The amount of B19 DNA in the sample was determined by dot blot analysis as described in the legend of Fig. 1A, and equivalent quantities of B19 DNA were analyzed by DNA hybridization after Southern transfer. The model of animal parvovirus replication (*19*) shows the characteristic molecular intermediates in the life cycle of these single-stranded viruses. Autonomous members of the family Parvoviridae initiate replication through a self-priming 3′ hairpin loop to generate duplex intermediate replication forms. Addition of nucleotides at the 3′ end (in a 5′ → 3′ direction) forms a complementary strand to produce the monomer replicative form. Further extension in the 5′ → 3′ direction leads to formation of the dimer replication form, consisting of two positive and two negative strands. Cleavage of this product generates new infectious virus. (B) Restriction enzyme digestion of B19 DNA from infected bone marrow cultures. DNA from nuclei and B19 virus was annealed under high salt conditions (*8*); undigested and Bam HI–digested samples were analyzed by DNA hybridization after Southern transfer (as in Fig. 1). The predicted fragments from Bam HI digestion of annealed duplex and replicative form duplex B19 DNA are shown below the radiographs. The 0.1-kb difference is based on structural differences between the hairpin and extended forms of the restriction fragments (*11*).

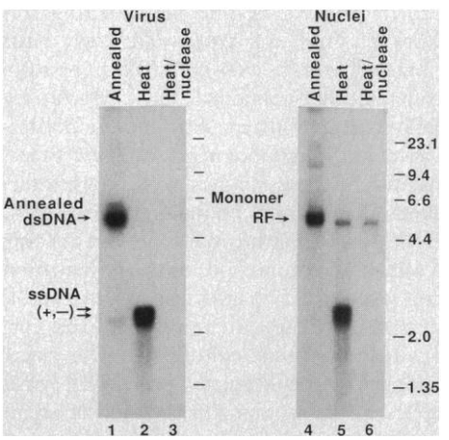

Fig. 4. Demonstration of the hairpin replicative form of B19 DNA in a snap-back experiment. DNA samples were prepared and annealed as described in the legends of Figs. 1 and 2 (lanes 1 and 4), heat-denatured at 95°C for 5 minutes and quick-chilled in ice (lanes 2 and 5), and subjected to mung bean nuclease digestion [2 U of enzyme per microgram of denatured DNA, 30°C for 30 minutes (lanes 3 and 6)], and analyzed by DNA hydridization after Southern transfer (as is in Fig. 1).

upon chilling these duplexes collapse into single-stranded DNA, which is susceptible to nuclease digestion. In contrast, while heating also separates the strands of the replicative forms, their covalent linkage through terminal hairpins leads to rapid reannealing after chilling; the resulting double-stranded DNA molecules are resistant to nuclease digestion (nicking of the replication forms would prevent snap-back, leading to the apparent difference in quantity of hairpin forms in Fig. 3 compared to Fig. 2B).

Inhibition of erythroid but not myeloid colony formation has been observed after infection of normal human bone marrow cells with B19 (*11*). A similar specificity of B19 for erythroid cell progenitors was demonstrated in suspension cultures (Table 1). Production of B19 was proportional to the erythroid content of the bone marrow cell samples. Replication of B19 was greatly enhanced by the addition of erythropoietin but only slightly increased by the use of conditioned media containing colony-stimulating factors and burst-promoting activity. These results indicate that the target cell of the B19 in suspension cultures is a precursor to mature erythrocytes, probably more responsive to erythropoietin than to factors operating on less mature hematopoietic progenitors.

A large number of cell lines have been tested unsuccessfully for their ability to propagate B19 virus. Dot blot analysis of DNA from B19-inoculated K562 (*14*) and HEL (*15*) erythroleukemia cell lines, even after hemin induction, failed to show the presence of B19 DNA within whole cells or nuclei (Fig. 1), despite the erythroid features of these cell types. However, virus obtained from human erythroid bone marrow cultures contained the characteristic B19 proteins as detected by immunofluorescence and immunoblotting, and the supernatants of these cultures were more infectious than serum containing virus (*10*). Bone marrow culture may represent the only feasible current method for the propagation and study of B19 parvovirus in vitro, and it may be safer than attempting to adapt parvoviruses to tissue culture (*9*). The target and site of replication of the B19 virus appear to be an immature cell in the erythroid lineage. Molecular analysis of suspension cultures should allow determination of the basis for the specificity of the B19 parvovirus for erythroid cells, evident from both culture and clinical observations. The tissue tropism of this virus may be utilizable in the construction of vectors specific to erythroid progenitors for the treatment of human hemoglobinopathies by stem-cell transfection.

REFERENCES AND NOTES

1. Y. E. Cossart, A. M. Field, B. Cant, D. Widdows, *Lancet* **1975-I**, 71 (1975).
2. J. R. Pattison *et al.*, *ibid.* **1981-I**, 664 (1981); G. R. Serjeant *et al.*, *ibid.* **1981-II**, 595 (1981).
3. M. J. Anderson *et al.*, *ibid.* **1983-I**, 1378 (1983).
4. D. G. White *et al.*, *ibid.* **1985-I**, 419 (1985); D. M. Reid, T. M. S. Reid, T. Brown, J. A. N. Rennie, C. J. Eastmond, *ibid.*, p. 422.
5. P. D. Knott, G. A. C. Welply, M. J. Anderson, *Br. Med. J.* **289**, 1660 (1984); T. Brown, A. Anand, L. D. Ritchie, J. P. Clewley, T. M. S. Reid, *Lancet* **1984-II**, 1033 (1984).
6. J. Summers, S. E. Jones, M. J. Anderson, *J. Gen. Virol.* **64**, 2527 (1983).
7. J. Clewley, *ibid.* **65**, 241 (1984).
8. S. Cotmore and P. Tattersall, *Science* **226**, 1161 (1984).
9. G. Siegl, in *The Parvoviruses*, K. I. Berns, Ed. (Plenum, New York, 1984), pp. 363–388.
10. K. Ozawa *et al.*, unpublished data.
11. P. P. Mortimer, R. K. Humphries, J. G. Moore, R. H. Purcell, N. S. Young, *Nature (London)* **302**, 426 (1983).
12. U. M. Saarinen *et al.*, *Blood* **67**, 1411 (1986).
13. New synthesis of B19 parvovirus in vitro was inferred from two other experiments (K. Ozawa, G. Kurtzman, N. Young, in preparation). Viral output into supernatant varied with the multiplicity of infection (MOI), and at low MOI 50× the input virus was present in culture fluids. In addition, [^{35}S]methionine-labeled capsid proteins were present in the particulate fraction after sucrose gradient sedimentation of culture supernatants.
14. C. B. Lozzio and B. B. Lozzio, *Blood* **45**, 321 (1980).
15. P. Martin and T. Papayannopoulou, *Science* **216**, 1233 (1982).
16. N. N. Iscove and F. Melchers, *J. Exp. Med.* **147**, 923 (1979).
17. Gift from P. Tattersall.
18. K. Ozawa *et al.*, *Biochem. Biophys. Res. Commun.* **130**, 257 (1985).
19. W. W. Hauswirth, in *The Parvoviruses*, K. I. Berns, Ed. (Plenum, New York, 1984), pp. 129–152.

20. We thank P. Tattersall for the generous gift of pYT103 and for helpful advice in the interpretation of these studies and M. Harrison for preparing the electron micrograph.

13 January 1986; accepted 28 May 1986

Calcium Rises Abruptly and Briefly Throughout the Cell at the Onset of Anaphase

MARTIN POENIE, JANET ALDERTON, RICHARD STEINHARDT, ROGER TSIEN

Continuous measurement and imaging of the intracellular free calcium ion concentration ($[Ca^{2+}]_i$) of mitotic and interphase PtK_1 cells was accomplished with the new fluorescent Ca^{2+} indicator fura-2. No statistically significant difference between basal $[Ca^{2+}]_i$ of interphase and mitotic cells was detected. However, mitotic cells showed a rapid elevation of $[Ca^{2+}]_i$ from basal levels of 130 n*M* to 500 to 800 n*M* at the metaphase-anaphase transition. The $[Ca^{2+}]_i$ transient was brief, lasting approximately 20 seconds and the elevated $[Ca^{2+}]_i$ appeared uniformly distributed over the entire spindle and central region of the cell. The close temporal association of the $[Ca^{2+}]_i$ transient with the onset of anaphase suggests that calcium may have a signaling role in this event.

THE ONSET OF ANAPHASE IS AN abrupt transition characterized by the separation of chromatids at the metaphase plate followed by the rapid displacement of chromosomes toward the poles. The localization of calcium-sequestering activity and calmodulin in the spindle region (*1, 2*), the alteration of metaphase transit times by manipulation of intracellular or extracellular calcium (*3, 4*), the sensitivity of microtubule polymerization to calcium (*5*), and the mitotic arrest caused by a variety of calmodulin inhibitors (*6, 7*), all point to a possible regulatory role for cytoplasmic calcium ions in mitosis. We previously reported measurements of intracellular free calcium ion concentration ($[Ca^{2+}]_i$) during the first cell division cycle of fertilized *Lytechinus pictus* eggs; we detected a brief calcium transient in close temporal proximity to the metaphase transition (*8*). However, since we could not resolve the chromosomes in these eggs, the exact timing of the metaphase-anaphase transition in relation to the calcium transient could not be determined. We also did not determine the spatial distribution of $[Ca^{2+}]_i$ during these measurements. Keith *et al.* (*9*) measured $[Ca^{2+}]_i$ in PtK_2 cells with quin-2 and did not detect a calcium transient, but reported that average $[Ca^{2+}]_i$ declined during mitosis (*9*). In another study Keith *et al.* found that calcium did rise at the poles during the metaphase-anaphase transition in *Haemanthus* cells (*10*).

Here we report the measurement of $[Ca^{2+}]_i$ during mitosis in PtK_1 cells with fura-2, a new fluorescent indicator of $[Ca^{2+}]_i$ (*11, 12*). Fura-2 signals increased $[Ca^{2+}]_i$ by an increase in the ratio of 350-nm to 385-nm excitation efficiency, which was quantified by either a photomultiplier

M. Poenie and R. Tsien, Department of Physiology-Anatomy, University of California, Berkeley, CA 94720. J. Alderton and R. Steinhardt, Department of Zoology, University of California, Berkeley, CA 94720.